Inorganic Chemistry

Article

pubs.acs.org/IC

Accommodating Unwelcome Guests in Inorganic Layered Hosts: Inclusion of Chloranil in a Layered Double Hydroxide

Dipak Dutta and Sukumaran Vasudevan*

Department of Inorganic and Physical Chemistry, Indian Institute of Science, Bangalore 560012, India

Supporting Information

ABSTRACT: The host–guest chemistry of most inorganic layered solids is limited to ion-exchange reactions. The guest species are either cations or anions to compensate for the charge deficit, either positive or negative, of the inorganic layers. Here, we outline a strategy to include neutral molecules like *ortho*- and *para*-chloranil, that are known to be good acceptors in donor–acceptor or charge-transfer complexes, within the galleries of a layered solid. We have succeeded in including neutral *ortho*- and *para*-chloranil molecules within the galleries of an Mg-Al layered double hydroxide (LDH) by using charge-transfer interactions with preintercalated *p*-aminobenzoate ions as the driving force. The *p*-aminobenzoate ions are introduced in the Mg-Al LDH via ion exchange. The intercalated LDH can adsorb *ortho*- and *para*-chloranil from chloroform solutions by forming charge-transfer complexes with the *p*-aminobenzoate anions present in the galleries. We use X-ray diffraction, spectroscopy, and molecular dynamics simulations to establish the nature of interactions and arrangement of the charge-transfer complex within the galleries of the layered double hydroxide.

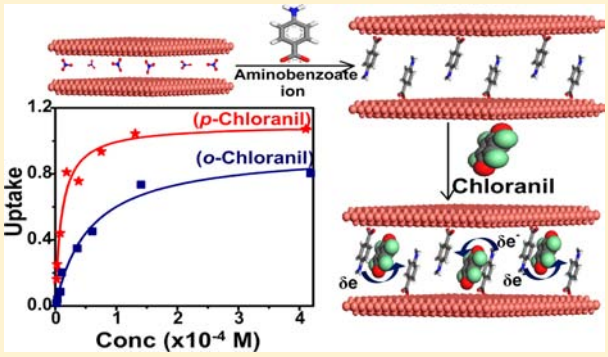

INTRODUCTION

Insertion of organic or organometallic guest species in inorganic host lattices offers an attractive route to hybrids in which complementary properties of the individual components are expressed in a single material. Layered solids in which guest species can access interlamellar space via the intercalation reaction provide some of the best studied examples of such systems.[1,2] In a majority of layered solids, that include the mica-type silicate clays,[3] the layered double hydroxides,[4,5] the divalent metal thiophosphates,[6] and metal(IV) phosphates and phosphonates,[1,7] etc., intercalation is driven either by oxidation–reduction, acid–base, or ion-exchange reactions. The interaction between host and guest is Coulombic, with the guest species compensating for the charge deficit, either positive or negative, of the inorganic layer. Guest species are consequently restricted to ionic or charged species and the subsequent host–guest chemistry of the intercalated solids restricted to the exchange of the interlamellar charged species for other ions; neutral molecular species that do not do so are generally unwelcome.

The host–guest chemistry of the layered hosts can, however, be extended to include nonpolar molecules by appropriate functionalization of the internal surface of the solid.[8,9] The strategy, so far, has been to convert the essentially hydrophilic interlamellar space of the inorganic solid to one that is hydrophobic such that nonpolar molecules can be accommodated by favorable dispersive interactions. This may be achieved, for example, by grafting to the inorganic sheets organic molecules, which can themselves act as hosts. Intercalation of surfactants,[10−13] cyclodextrins (CD),[14−18] and crown-ethers[19] in layered solids can generate new host structures whose host–guest chemistry is not limited to that of the parent inorganic solid. It is well-established that anchoring of long-chain surfactant molecules to the walls of the galleries, to form intercalated bilayers, allows for the solubilization of a wide variety of neutral organic molecules in the hydrophobic interior of the bilayer.[20−26] Similarly, modified CDs have been successfully intercalated in montmorillonite clays,[27] zirconium phosphates,[14] and layered double hydroxides[15,18] to create a new generation of host structures wherein guest molecules may be included within the hydrophobic cavities of the anchored CD.[28−34]

Here, we have adopted a different approach. We use charge-transfer interactions to force the insertion of a neutral acceptor molecule within the galleries of a layered host. To do so, we first functionalize the layered solid by anchoring donor groups to the gallery walls. The layered host that we have chosen for this study is an Mg-Al layered double hydroxide (LDH). The LDHs, or anionic clays, consists of $[Mg_{1-x}Al_x(OH)_2]^{x+}$ positively charged brucite-like sheets constructed from edge-sharing $Mg(OH)_6$ and $Al(OH)_6$ octahedra. The positive charge of the layers is compensated by interlayer anions that are usually hydrated. The interlayer anion can be exchanged for other inorganic or organic anions and this property of the LDHs has been widely investigated.[4] Aniline–chloranil,

Received: February 9, 2012
Published: July 19, 2012

   dx.doi.org/10.1021/ic3002948 | Inorg. Chem. 2012, 51, 8064–8072

wherein partial transfer of charge from aniline is responsible for charge-transfer complex formation, was the donor−acceptor pair chosen for this study.[35,36] The donor was introduced into the galleries of Mg-Al LDH as *p*-aminobenzoate anions by a conventional ion-exchange intercalation. We show here that neutral *o*- and *p*-chloranil molecules may be driven into the galleries of the layered solid by charge-transfer complex formation with the intercalated *p*-aminobenzoate anions. We use diffraction, spectroscopy, and molecular dynamics simulations to establish the nature of interactions and arrangement of the charge-transfer complex within the galleries of the layered double hydroxide.

EXPERIMENTAL SECTION

Materials and Methods. $Mg_{1-x}Al_x(OH)_2(NO_3)_x$−(Mg-Al LDH-$NO_3$) was prepared by coprecipitation by dropwise addition of known volumes of aqueous $Mg(NO_3)_2$ (0.04 M) and $Al(NO_3)_3$ (0.02 M) into NaOH at a constant pH of 8, under a N_2 atmosphere, following reported procedures.[37] The resulting white precipitate was aged for 24 h prior to washing with decarbonated water. *p*-Aminobenzoate (AB) ions were introduced within the galleries of Mg-Al LDH by ion-exchanging the NO_3 ions in (Mg-Al LDH-NO_3). The ion-exchange reaction was carried out by stirring Mg-Al LDH-NO_3 with an aqueous solution of potassium *p*-aminobenzoate for 24 h at room temperature. The ion-exchanged $Mg_{1-x}Al_x(OH)_2(AB)_x$ was filtered and washed to remove excess AB ions. Completion of the ion exchange of AB ions was confirmed by infrared spectroscopy that showed an absence of the characteristic NO_3 band at 1384 cm^{-1} in the ion-exchanged samples. The AB ion stoichiometry in the intercalated Mg-Al LDH-AB was established from C,H,N elemental analysis (Heraeus CHN-O-RAPID elemental analyzer) (C% = 20.54%, H% = 4.63%). Mg/Al ratios in the LDH were determined by inductively coupled plasma spectroscopy (iCAP 6500-Thermo Scientific) and the water content by TGA (Netzsch, Model TG 209 F1 Iris thermal analyzer at 10°/min heating rate). The composition of the starting (Mg-Al LDH-NO_3) was $Mg_{0.670}Al_{0.333}(OH)_2(NO_3)_{0.332}\cdot 0.53H_2O$ and that of Mg-Al LDH-AB was $Mg_{0.670}Al_{0.333}(OH)_2\ (AB)_{0.329}\cdot 0.82H_2O$.

Powder X-ray diffraction (XRD) patterns were recorded in the Bragg−Brentano geometry on a Bruker AXS D8 ADVANCE diffractometer (40 kV, 30 mA), using Cu Kα radiation (λ = 1.54 Å). In the region of 1°−5°, a scintillation detector was used while, at higher angles, a LynxEye solid-state detector was used. Fourier transform infrared (FT-IR) spectra were recorded in the transmittance mode as KBr pellets on a Perkin−Elmer Spectrum One spectrometer and in the attenuated total reflectance mode on a Bruker ALPHA-P spectrometer, both operating at a resolution of 4 cm^{-1}. FT-Raman spectra were recorded on a Bruker IFS spectrometer, using an Nd:YAG (λ = 1064 nm) laser for excitation. Spectra were recorded at a resolution of 4 cm^{-1} with an unpolarized beam, using an Al sample holder. Laser power was kept at ∼15 mW. Low-temperature Raman spectra were recorded on a Renishaw inVia confocal Raman spectrometer coupled to a Leica microscope with a 20× objective in the backscattering geometry, using a freeze-drying cryo-stage (FDCS 196, Linkam Scientific Instruments) equipped with a liquid nitrogen cooling system (LNP94/2, Linkam). Argon-ion laser of wavelength 514.5 nm was used as a source. The spectra were recorded in five acquisitions of 20 s accumulations and a laser power of 0.5 mW at the sample. Absorption spectra in solution were recorded at room temperature on a Perkin−Elmer Lambda 35 ultraviolet−visible (UV-vis) spectrophotometer with a slit width of 2 nm and a scan speed of 240 nm/min. Absorption spectra for the solid samples were recorded in the diffused-reflectance mode in the range of 190−1200 nm on a Perkin−Elmer Lambda 750 spectrophotometer, using a 60-mm integrating sphere.

Adsorption Measurements. Adsorption isotherms for the uptake of *ortho*- and *para*-chloranil were measured in the batch mode. Weighed quantities of Mg-Al LDH-AB, typically 100 mg, were equilibrated with 10 mL of differing concentrations of *ortho*- and *para*-chloranil in chloroform at room temperature for 24 h. The LDH samples that are off-white in color turn to dark green within a few minutes. The concentrations of included chloranil was obtained as the difference in concentration of chloranil in the solution before and after the equilibrating with Mg-Al LDH-AB. Chloranil concentrations were obtained by monitoring the intensity of the 370-nm band of *p*-chloranil (the 455-nm band for *o*-chloranil) in the UV−vis spectra.

Molecular Dynamics Methodology. Molecular dynamics (MD) simulations were used to understand the arrangement of guest species in the galleries of Mg-Al LDH. Simulations were first performed on the *p*-aminobenzoate intercalated Mg-Al LDH (Mg-Al LDH-AB) and subsequently *ortho*- and *para*-chloranil molecules were introduced, in the galleries of the simulation derived structure of Mg-Al LDH-AB and the calculations repeated. The first step in running an MD simulation of a layered solid is building the structure in the computer by assigning positions to individual atoms. The structure of the *p*-aminobenzoate intercalated Mg-Al LDH was generated by creating the structure of the inorganic Mg-Al LDH host and the organic guest separately and then putting them together. The Mg-Al LDH host lattice was built using atomic coordinates from the previously reported crystal structure of hydrotalcite, $[Mg_4Al_2(OH)_{12}](CO_3)\cdot 3H_2O$ (Al/Mg = 0.5), whose crystal structure had been refined in a trigonal unit cell with space group $R\bar{3}m$ and lattice parameters $a = b$ = 3.046 Å and c = 22.81 Å.[38] The Mg-Al LDH structure was generated from that of hydrotalcite that had a unit-cell composition of $Mg_2Al(OH)_6(CO_3)\cdot 0.5H_2O$. The interlamellar carbonate ions and the water molecules were removed. A large unit cell (LUC) was then created by a 3×3 translation of the unit cell in the *a*- and *b*-directions. The lattice parameters of this LUC were $a = b$ = 9.138 Å, and each cell had three layers. The composition of this LUC was $Mg_{18}Al_9(OH)_{54}$. At this stage, all the metal ions were treated as equivalent, so that, in effect, the composition of the LUC was $Mg_{27}(OH)_{54}$ and each layer had composition $Mg_9(OH)_{18}$ formed by edge-sharing $Mg(OH)_6$ octahedra.

The present study required the building of Mg-Al LDH structures with x = 0.33. The distribution of Mg and Al within the LDH layers was based on a Monte Carlo study of the ordering of A^{m+} and B^{n+} ($m \neq n$) ions in an $A_{(1-x)}B_x$ alloy on a 2D triangular lattice at different compositions.[39,40] To obtain the required Mg/Al ratio, the Mg atoms were substituted by Al atoms in unit increments to obtain $Mg_6Al_3(OH)_{18}$ (x = 0.33). The conversion to a 6×6×1 giant super cell leads to the composition $Mg_{24}Al_{12}(OH)_{72}$. The lattice was then dilated along the *c*-direction (interlayer axis) to accommodate the guest AB ions and water molecules. The AB ions were then placed randomly in the interlamellar region of the LDH, such that they formed a bilayer arrangement. Overall, 12 AB monovalent anions were introduced to compensate for the positive charge of the $Mg_{24}Al_{12}(OH)_{72}$ layers. In addition, 30 water molecules were also included in the interlamellar space. This would correspond to a water to intercalated AB ion molar ratio of 2.5, in agreement with the TGA data (see Figure S1 in the Supporting Information).

The bonding interactions were modeled by using a composite force field to reflect the hybrid nature of the organic−inorganic system. The inorganic sheets require a hard potential while the intercalated *p*-aminobenzoate ions require a softer potential to reflect their dynamic nature. The potential energy for the inorganic layers was modeled using the universal force field (UFF).[41] The aromatic AB ions and water molecules were modeled using the modified Dreiding force field.[42−44] Charges on the atoms of the inorganic lattice were obtained by density functional theory (DFT) calculation, using the DMol^3 module of Materials Studio package.[45] A double numerical with polarization (DNP) basis set with the Perdew−Wang (PW91) functional was used to calculate the eigenstates and eigenvectors. A Mulliken population analysis was then performed to obtain the charges on individual atoms. The AB ions have a unit negative charge. The charges on the individual atoms of AB ion were computed using Gaussian 09.[46] Charges were obtained by a Mulliken population analysis of the molecular orbitals calculated by the Hartree−Fock method, using the 6-31G** basis set. The charges on individual atoms of the AB ion are summarized in the Supporting Information (Figure S2). For water, the initial geometry and atomic charges (+0.417 for H

dx.doi.org/10.1021/ic3002948 | Inorg. Chem. 2012, 51, 8064−8072

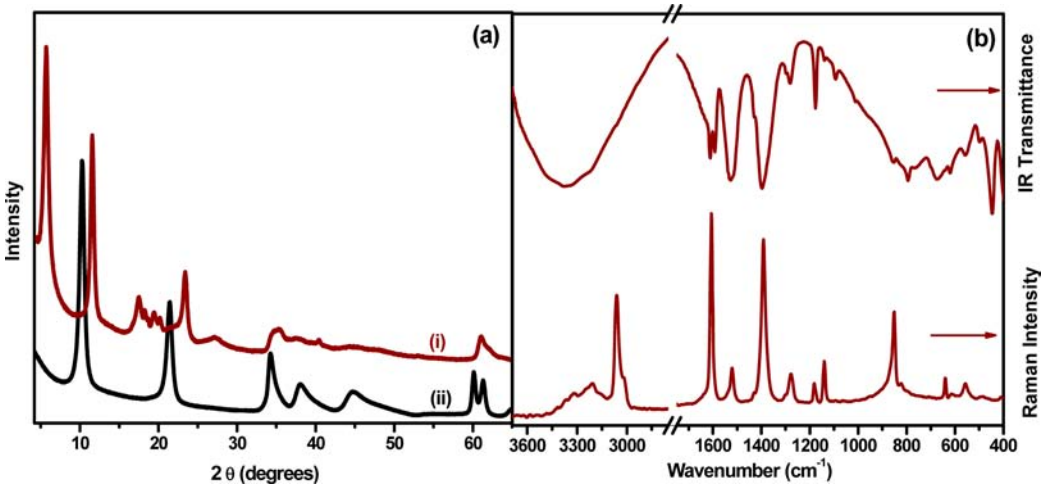

Figure 1. (a) X-ray diffraction patterns of Mg-Al LDH-AB (spectrum i) and Mg-Al LDH-NO_3 (spectrum ii). (b) Infrared and Raman spectra of Mg-Al LDH-AB.

and −0.834 for O) were taken from the TIP3P specialized water force field.[47] The total nonbonded potential interaction energy of the simulated system consisted of long-range Coulombic interactions between partial atomic charges, computed using the Ewald summation technique with an accuracy of 10^{-6} kcal/mol. The cutoff distance for van der Waals interactions was kept at 12 Å.

Two-nanosecond (2-ns) MD simulations were performed on the AB ion intercalated Mg-Al LDH at a temperature of 298 K. MD calculations were performed using the Forcite+ module of the Materials Studio package.[45] The velocity-Verlet integrator method was used to compute the positions and velocities of atoms. Simulations were initiated on a constant composition, isothermal−isobaric (NPT) ensemble with a time step of 1 fs. The temperature of the ensemble was maintained by the velocity scale thermostat with a temperature difference window of 10 K.[48] The equivalent hydrostatic pressure was set to 0.0001 GPa (∼1 atm). Periodic boundary conditions were applied in three dimensions, so that the simulation cell is effectively repeated infinitely in each direction. The simulations were initiated from a geometry where the interlayer separation was at least 1.5 times greater than the experimental interlayer spacing. Typically, convergence to an equilibrium value at each step was realized within the first 50 ps.

Chloranil molecules were then introduced in the galleries of the simulation-derived Mg-Al LDH-AB structure. Chloranil molecules were placed randomly between the anchored AB ions with no fixed orientation, with respect to the AB ions. The number of *para*-chloranil molecules introduced was varied from 1 to 12, corresponding to molar ratios of *para*-chloranil to intercalated AB ions of 0.1 to 1. For *ortho*-chloranil, the number of molecules was varied from 1 to 9, corresponding to molar ratios of 0.1 to 0.75. Twelve (12) water molecules were also introduced in the galleries, to maintain an AB-ion-to-water molar ratio of 1. This ratio was obtained from a TG analysis of Mg-Al LDH-AB with included *o*- and *p*-chloranil molecules (see Figure S1 in the Supporting Information). Prior to their introduction in the galleries of the Mg-Al LDH-AB structure, the geometry of the chloranil molecules was optimized using the Gaussian 09 package.[46] The charges on the individual atoms of the *o*- and *p*-chloranil molecules were obtained by a Mulliken population analysis of the molecular orbitals calculated by the Hartree−Fock method, using a 6-31G** basis set. After introduction of the *o*- and *p*-chloranil molecules, the Mg-Al LDH-AB structure with the chloranil molecules was charge-equilibrated. Two-nanosecond (2-ns) NPT MD simulations were then performed at 298 K with a time-step of 1 fs. Similar to the previous simulations, a composite force field was used. The inorganic layers were modeled using the universal force field (UFF),[41] while the AB ions and chloranil molecules were modeled using the modified Dreiding force field.[42−44]

RESULTS AND DISCUSSION

Intercalation of *p*-Aminobenzoate (AB) Anions. The *p*-aminobenzoate anion was introduced within the galleries of Mg-Al LDH by ion exchanging the NO_3 ions in Mg-Al LDH-NO_3 with AB ions. Intercalation of the AB anions is accompanied by a dilation of the lattice from 8.9 Å to 15.2 Å (see Figure 1a). The interlayer spacing is identical to the value reported for the AB ion intercalated in Zn-Al LDH (15.19 Å).[49] Completion of the ion exchange was established by the absence of 00*l* peaks with an interlayer spacing of 8.9 Å, corresponding to Mg-Al LDH-NO_3. There is a small shift (0.9°) in the position of the 110 reflection, compared to Mg-Al LDH-NO_3. However, because there is no change in the Mg/Al ratio upon intercalation of the AB ion, no significance is attached to it. Corroborative evidence for completion of exchange was also provided by the infrared and Raman spectra of Mg-Al LDH-AB (Figure 1b); the characteristic ν_{asym} stretching band of NO_3 at 1384 cm^{-1} is absent in the infrared spectrum. The more significant features in the infrared spectrum of Mg-Al LDH-AB (Figure 1b) are the aromatic C−C stretch of the AB ion at 1611 cm^{-1}, the N−H asymmetric and symmetric bending at 1592 and 1176 cm^{-1}, respectively, and the antisymmetric and symmetric stretching modes of the carboxylate group of the AB ion that appear at 1528 and 1397 cm^{-1}, respectively. In the corresponding Raman spectrum the intense band at 3062 cm^{-1} is assigned to the aromatic C−H stretching mode and the 1607 cm^{-1} band is assigned to the N−H scissoring mode, while the 1391 and 1277 cm^{-1} bands are assigned to the COO^- symmetric stretch and C−N stretch, respectively. Details of the band positions and assignments in the infrared and Raman spectra of Mg-Al LDH-AB are provided in the Supporting Information (Table S1). The positions of the bands in the infrared and Raman spectra of Mg-Al LDH-AB are identical to that of the *p*-aminobenzoate ion in its salts (see the Supporting Information) and indicate that the structural and geometrical integrity of the AB ion is preserved upon intercalation. The length of the AB ion is 7.8 Å, while the available interlamellar space in the intercalated Mg-Al LDH-AB obtained after subtracting the thickness of the Mg-Al LDH sheet (4.8 Å)[37] is 10.4 Å. This suggests that the AB ions may be arranged as partially interdigitated bilayers. This was confirmed by MD simulations described in a later section.

dx.doi.org/10.1021/ic3002948 | *Inorg. Chem.* 2012, 51, 8064−8072

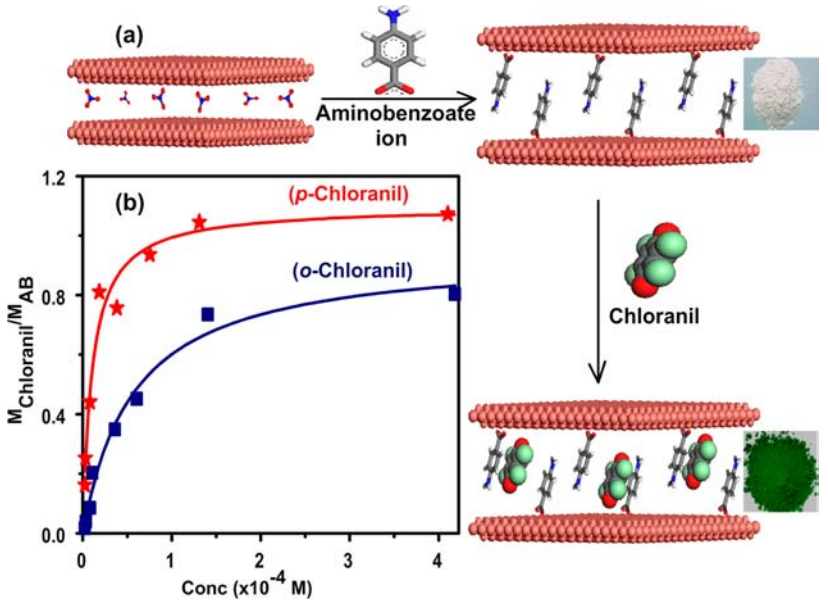

Figure 2. (a) Schematic illustration of the functionalization of the Mg-Al double hydroxide layers by exchange of the interlayer nitrate anions with *p*-aminobenzoate ions, followed by inclusion of neutral chloranil. (b) Equilibrium uptake isotherm of chloranil, from a chloroform solution, by the functionalized Mg-Al LDH-AB. The uptake is expressed as the molar ratio of included chloranil to intercalated AB ions.

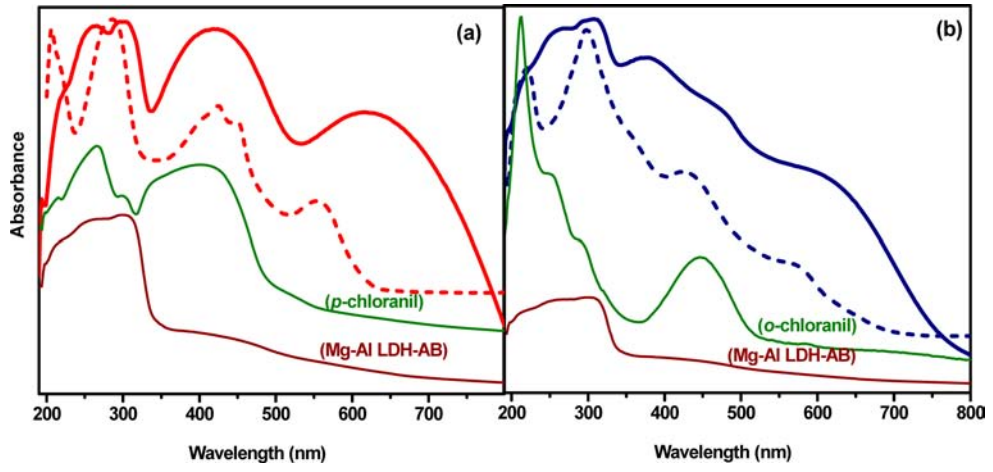

Figure 3. Ultraviolet−visible (UV-vis) spectra of (a) Mg-Al LDH-(AB·*p*-chloranil) and (b) Mg-Al LDH-(AB·*o*-chloranil). The corresponding solution spectra of the 1:1 AB-chloranil charge-transfer complex in ethanol is shown in dashed lines.

Insertion of Chloranil. *Adsorption Isotherm.* The donor intercalated Mg-Al LDH-AB adsorbs neutral chloranil molecules from solution, changing in color from off-white to deep green (see Figure 2a). The adsorption isotherm for the uptake of *para*- and *ortho*-chloranil from their chloroform solutions by Mg-Al LDH-AB at room temperature is shown in Figure 2b. The adsorption is expressed as the molar ratio of adsorbed chloranil to anchored AB ions and is plotted against the equilibrium concentration of chloranil in solution. The corresponding Mg-Al LDH-NO_3 shows no uptake of either *o*- or *p*-chloranil or color change, indicating that the isotherms in Figure 2b are due to inclusion of chloranil by charge transfer complex formation with the intercalated AB ions. The adsorption isotherms (Figure 2b) resemble a Langmuir isotherm with the curve flatting out at a molar ratio of 1.0 for *p*-chloranil and 0.80 for *o*-chloranil. In solution, the formation of 1:1 AB:chloranil ion charge-transfer complexes are known[35,36] and the isotherms (Figure 2b) indicates a similar stoichiometric ratio in the Mg-Al LDH-(AB·*p*-chloranil), although the question of the lower uptake of *ortho*-chloranil would have to be addressed.

Electronic Spectra. The insertion of chloranil in Mg-Al LDH-AB is accompanied by a change in color. The UV-vis spectra show an additional feature at 618 nm for Mg-Al LDH-(AB·*p*-chloranil) and at 620 nm for Mg-Al LDH-(AB·*o*-chloranil). This feature may be assigned to the included charge-transfer complex. The spectra along with that of the individual components, Mg-Al LDH-AB, and chloranil, are shown in Figure 3. The corresponding spectra of the 1:1 AB-*p*-chloranil and AB-*o*-chloranil complexes in solution are also shown in Figure 3. It may be seen that the feature assigned to the charge-transfer complex in the spectra of Mg-Al LDH-(AB·*p*-chloranil) and Mg-Al LDH-(AB·*o*-chloranil) is red-shifted, in comparison to the solution spectra. The extent of the red shift is 63 nm for the *p*-chloranil complex and 50 nm for *o*-chloranil. The spectral features that appear below 500 nm may be assigned to the individual components, and they appear

dx.doi.org/10.1021/ic3002948 | *Inorg. Chem.* 2012, 51, 8064−8072

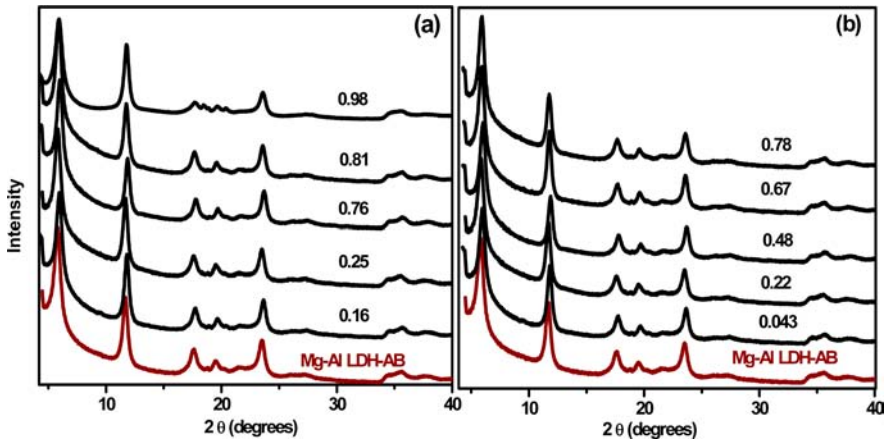

Figure 4. X-ray diffraction (XRD) patterns of (a) Mg-Al LDH-(AB·*p*-chloranil) and (b) Mg-Al LDH-(AB·*o*-chloranil) at different molar ratios of included chloranil to intercalated AB ions.

at almost the same wavelengths as in Mg-Al LDH-AB and chloranil.

X-ray Diffraction. The X-ray diffraction (XRD) patterns of the chloranil included Mg-Al LDH-(AB·*p*-chloranil) and Mg-Al LDH-(AB·*o*-chloranil) at different molar ratios of included chloranil to intercalated AB ions are shown in Figure 4. Surprisingly, there is no change in the interlayer spacing from that of the parent Mg-Al LDH-AB, even at the highest concentration of included chloranil. For Mg-Al LDH-(AB·*p*-chloranil) at a chloranil:AB ratio of 1.0, the interlayer spacing is 15.15 Å, while that of the starting Mg-Al LDH-AB is 15.2 Å. The obvious question then arises as to whether the AB-chloranil charge-transfer complex is formed within the galleries or exists outside the layers. However, the latter may be ruled out, because the presence of the AB anions within the galleries is required for charge neutrality to be maintained. It may be recalled that the Mg-Al LDH layers are positively charged and if the charge-compensating AB ions are not present would lead to a structural collapse. The XRD patterns of Mg-Al LDH-(AB·*p*-chloranil) and Mg-Al LDH-(AB·*o*-chloranil) in Figure 4 clearly indicate that this is not so. The possibility of the green color of the material due to partial deintercalation of AB ions and subsequent charge-transfer complex with chloranil on the exterior of the crystallites can also be ruled out, from the adsorption isotherm data, which indicated an uptake of a chloranil molecule for every intercalated AB ion. The absence of any lattice expansion on inclusion of chloranil is puzzling. The composition of the Mg-Al LDH used in the present study has the highest ion-exchange capacity among the Mg-Al LDHs and, consequently, the concentration of preintercalated AB ions is reasonably large; however, still, the inclusion of chloranil, forming a 1:1 chloranil-AB complex, occurs with no lattice dilation. However, note that there is, in principle, sufficient space (155.3 $Å^3$) available in the galleries of Mg-Al LDH-AB, after subtracting the van der Waals volume occupied by the AB ions (131.3 $Å^3$) and water molecules (23.36 $Å^3$), to accommodate a chloranil molecule for each intercalated AB ion. The van der Waals volumes of *p*-chloranil and *o*-chloranil are 145.0 and 153.7 $Å^3$, respectively.

Raman Spectra: The Extent of Charge Transfer. The Raman spectra of Mg-Al LDH-(AB·*p*-chloranil) and Mg-Al LDH-(AB·*o*-chloranil), along with that of the parent Mg-Al LDH-AB, are shown in Figure 5. The additional bands seen in the spectra of the included compounds are due to the presence

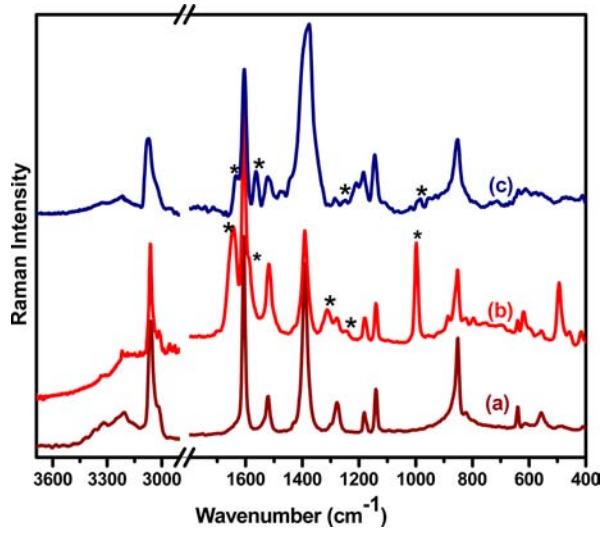

Figure 5. Raman spectra of (a) Mg-Al LDH-AB, (b) Mg-Al LDH-(AB·*p*-chloranil), and (c) Mg-Al LDH-(AB·*o*-chloranil). The molar ratio of included *para*-chloranil to intercalated AB ions is 0.8 (0.6 for *ortho*-chloranil). The bands of the included chloranil are indicated.

of chloranil. A detailed assignment of the bands and their positions is provided in the Supporting Information (Tables S2 and S3). Here, we focus on the chloranil C═O stretching and C═C antisymmetric stretching modes that are known to be sensitive to the average molecular charge, ς, of chloranil in a charge transfer complex.[50] In Mg-Al LDH-(AB·*p*-chloranil), these bands appear at 1643 and 1588 cm^{-1}, while in Mg-Al LDH-(AB·*o*-chloranil), the peak at 1637 cm^{-1} is assigned to the C═O stretching mode while the peak at 1562 cm^{-1} is ascribed to the ν_{asym}(C═C) mode.

The change in the vibrational frequency of the chloranil C═O bond with ionicity (ς) is well-documented; a frequency shift of ~160 cm^{-1} while going from the neutral molecule to the radical anion has been reported and a simple linear relation between the C═O stretching frequency (ν_{CO}) and the ionicity (ς) has been proposed.[51−53]

$$\nu_{CO} = 1685 - 160\varsigma$$

Using this relationship, a ν_{CO} value of 1643 cm^{-1} for *p*-chloranil in Mg-Al LDH-(AB·*p*-chloranil) would correspond to a value of 0.26 for ς while a ν_{CO} value of 1637 cm^{-1} would correspond to

dx.doi.org/10.1021/ic3002948 | *Inorg. Chem.* 2012, 51, 8064−8072

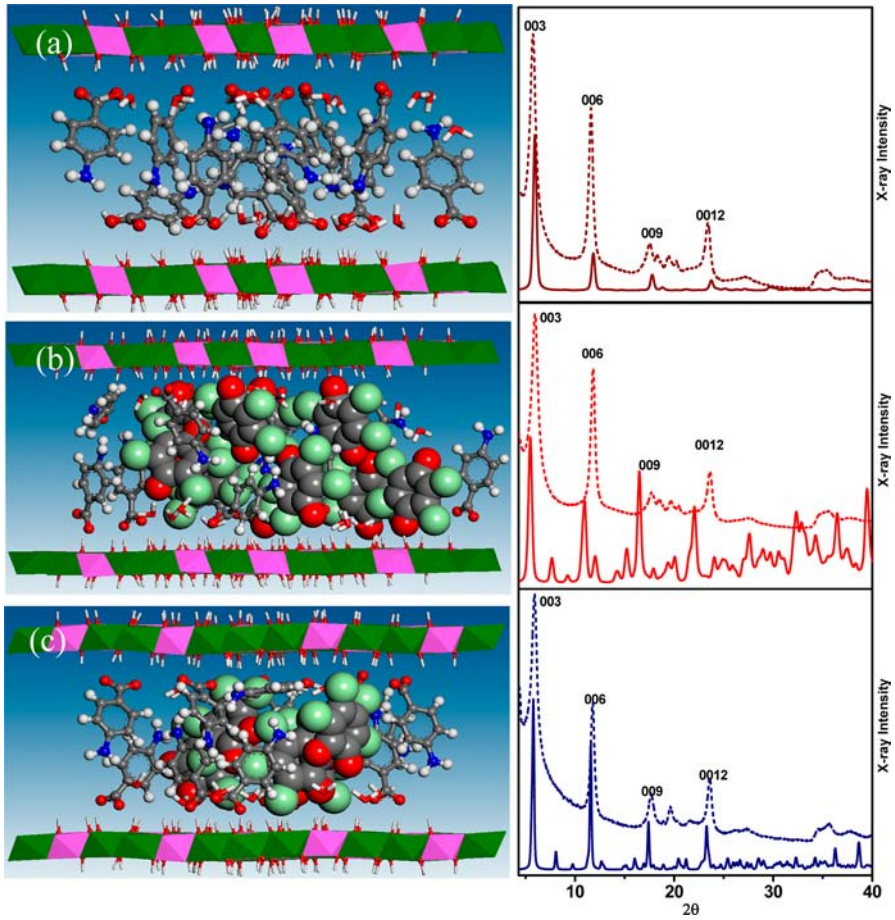

Figure 6. Snapshot of the MD simulated structure of (a) Mg-Al LDH-AB, (b) Mg-Al LDH-(AB·*p*-chloranil), and (c) Mg-Al LDH-(AB·*o*-chloranil). The snapshots are for a molar ratio of *para*-chloranil:AB of 0.83 and *ortho*-chloranil:AB ratio of 0.42. Color code: dark green = magnesium, magenta = aluminum, dark gray = carbon, light gray = hydrogen, red = oxygen, light green = chlorine, and blue = nitrogen. AB ions are represented by a ball-and-stick model, chloranil is represented by a space-filling model, and water is represented by a stick model. The panels on the right-hand side show the corresponding calculated (solid line) and experimental (dashed line) diffraction patterns.

an ionicity value of 0.28 in Mg-Al LDH-(AB·*o*-chloranil). The Raman spectra indicate that the extent of charge transfer from the intercalated AB ion to the included chloranil is comparable for the *ortho*- and *para*-isomers.

Molecular Dynamics. In order to understand how the intercalated and included molecules are arranged within the galleries of the Mg-Al LDH, MD simulations were performed on the intercalated Mg-Al LDH-AB in the presence and absence of included chloranil molecules. The objectives were 2-fold: (1) to investigate the arrangement of the intercalated AB ions in the galleries of the LDH consistent with the observed interlayer spacing of Mg-Al LDH-AB, and (2) to determine if the simulations could reproduce the experimental observation that the inclusion of chloranil molecules occurs with no change in the interlayer spacing of Mg-Al LDH-AB. Constant composition, isothermal–isobaric (NPT) simulations were performed on the AB ion intercalated Mg-Al LDH at 300 K. Subsequently, either the *o*- or *p*-chloranil molecule was introduced in the simulation-derived structure of Mg-Al LDH-AB and, after charge equilibration, the simulations repeated. Simulations were performed for a range of chloranil:AB molar ratios for both *para*- and *ortho*-chloranil. The total simulation time was 2 ns. The results showed that equilibrium values for the crystallographic parameters and thermodynamic quantities such as the potential energy were generally reached within the first 50 ps. Equilibrium values of the lattice parameters were judged to have been reached when these quantities fluctuate around their average values, which remain constant over time. Equilibrium values of the lattice parameters and thermodynamic quantities were also checked by repeating the simulations with a different starting orientation of the intercalated AB ions and chloranil molecules as well as interlayer spacing. Convergence to similar lattice parameters and properties from different initial values is a good indicator that equilibrium has occurred. Interlayer spacings were calculated by averaging over the last 10 ps of the simulation.

A snapshot of the equilibrium simulated structure of Mg-Al LDH-AB is shown in Figure 6a, and the calculated and experimental diffraction patterns are shown in the panel on the righthand side. The patterns are quite similar, and the *d*-spacing of 15.0 Å from simulation is in good agreement with the experimental value of 15.2 Å. The snapshot of the Mg-Al LDH-AB structure shows that the intercalated AB ions are arranged as interdigitated bilayers with the COO^- group close to the −OH of the layer. The water molecules are located in close proximity to the carboxylate of the AB ions. The plane of the AB ions is not normal to the layer but is tilted away from the normal by an angle of ∼15°. The MD simulations also indicate that the structure of the intercalated AB ion remains the same as that outside. This is consistent with the infrared and Raman

dx.doi.org/10.1021/ic3002948 | *Inorg. Chem.* 2012, 51, 8064–8072

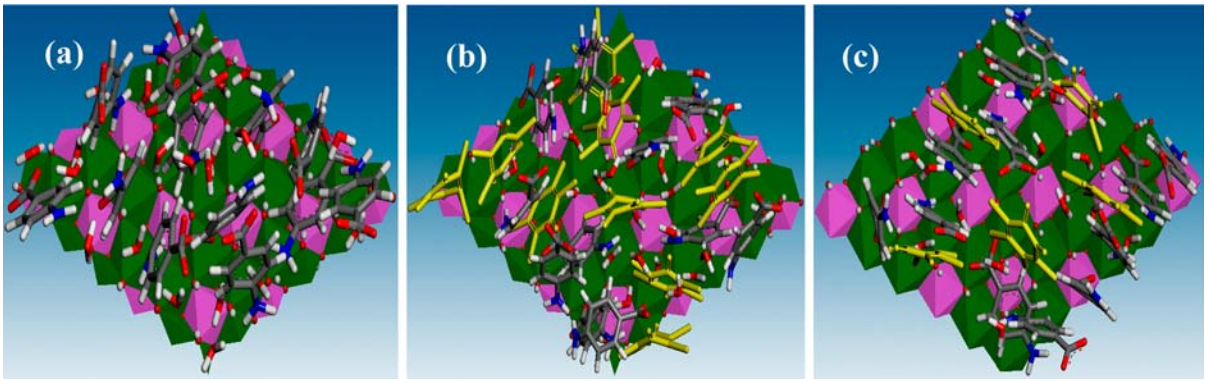

Figure 7. Snapshot of the MD simulated structure of (a) Mg-Al LDH-AB, (b) Mg-Al LDH-(AB·*p*-chloranil), and (c) Mg-Al LDH-(AB·*o*-chloranil) viewed down the interlayer normal. The snapshots are for a molar ratio of *para*-chloranil:AB of 0.83 and *ortho*-chloranil:AB ratio of 0.42. The *para*- and *ortho*-chloranil molecules are shown in yellow. For clarity, the top Mg-Al LDH layer has been removed.

data of Mg-Al LDH-AB (Figure 1b) that showed the vibration band positions to be identical to that of the AB ion in its salts.

Chloranil molecules were inserted in the equilibrium simulated structure of Mg-Al LDH-AB, between the intercalated AB ions but with no particular orientation with respect to the AB ions. As mentioned previously, charges on the *o*- and *p*-chloranil molecules were calculated using Gaussian 09 prior to insertion, and, subsequently, the entire structure charge were equilibrated and NPT MD simulations were performed. The number of included chloranil molecules in the simulation was such that the molar ratio of *para*-chloranil:AB varied from 0 to 1 while for *ortho*-chloranil:AB the ratio varied from 0 to 0.75. Snapshots of the equilibrium simulated structures of the included *para*- and *ortho*-chloranil are shown in Figures 6b and 6c. The simulations showed that interlayer spacing varied only marginally with increasing chloranil:AB ion ratio. For included *para*-chloranil, the interlayer spacing changed from 15.0 Å at a molar ratio of 0.1 to 15.94 Å for a ratio of 1.0. For included *ortho*-chloranil, the spacing changed from 15.0 Å at a ratio of 0.1 to 15.77 Å at a ratio of 0.75 (see Figure S3 in the Supporting Information). The experimental diffraction patterns had shown no change in the interlayer spacing from that of Mg-Al LDH-AB (15.2 Å) for all chloranil:AB ratios. It may be seen that the interlayer spacing of the calculated diffraction pattern at the extreme ratios is quite similar to the experimental XRD patterns.

The included chloranil molecules are oriented with their molecular planes approximately parallel to that of the tethered AB ions. A snapshot of the simulated structures viewed down the interlayer normal (Figure 7) shows that it is indeed possible to accommodate chloranil molecules in the Mg-Al LDH-AB structure without any lattice dilation. An interesting feature of the MD simulations of the Mg-Al LDH-(AB·*o*-chloranil) structure was the observation that it was not possible to exceed a *ortho*-chloranil:AB molar ratio of 0.75; the excess *ortho*-chloranil molecules were ejected from the interlamellar region. These observations may be understood from the fact that molar volume associated with the ortho isomer is larger than that of the para isomer. It thus appears that the number of included chloranil molecules is limited to a concentration that can be accommodated without any drastic change in the interlayer spacing from that of Mg-Al LDH-AB. Simulations provide an explanation for the adsorption isotherms (Figure 2) that showed a lower uptake for *ortho*-chloranil, compared to *para*-chloranil. In summary, the MD simulations reproduce the essential features of the experimental observations that chloranil molecules can be included within the AB ion intercalated Mg-Al LDH without any significant change in the interlayer spacing.

CONCLUSIONS

The layered double hydroxides or anionic clays consist of positively charged brucite-like inorganic sheets with exchangeable anions in the interlamellar space. The presence of negatively charged interlamellar species is a must for charge neutrality to be preserved and, consequently, the host−guest chemistry of these layered hosts is limited to ion-exchange reactions; neutral molecules are clearly unwelcome. Here, we adopt a new strategy to include neutral molecules such as *ortho*- and *para*-chloranil, which are known to be good acceptors in donor−acceptor or charge-transfer complexes. We first functionalize the layered double hydroxide by intercalating *p*-aminobenzoate anions. The intercalated *p*-aminobenzoate anions play a dual role, first by compensating for the deficit charge of the layers and second as electron donor groups, because of the presence of their nitrogen functionality. We show here that neutral chloranil molecules can be adsorbed from their chloroform solutions by forming charge-transfer complexes with the *p*-aminobenzoate anions in the galleries of the Mg-Al LDH. We have characterized the intercalated and included compounds by X-ray diffraction, adsorption measurements, spectroscopy, and molecular dynamics (MD) simulations.

p-Aminobenzoate (AB) anions were intercalated by ion-exchanging the NO_3 groups in Mg-Al LDH-NO_3. The intercalated Mg-Al LDH-AB has an interlayer spacing of 15.2 Å. MD simulations indicate that this lattice spacing can be defined by a bilayer arrangement with the AB ions tilted 15° away from the normal. Vibrational spectroscopy and MD simulations confirm that the structure of the intercalated AB ions is identical to that in salts of the AB ion. Neutral *ortho*- and *para*-chloranil molecules have been included in the galleries of Mg-Al LDH-AB by adsorption from their chloroform solutions. Adsorption isotherms for both isomers are Langmuir-like but the maximum uptakes differ. The molar ratio of chloranil to intercalated AB at saturation is 1.0 for the *para* isomer and 0.80 for the *ortho*. The inclusion of chloranil is accompanied by a change in color from off-white to dark green and the ultraviolet−visible (UV-vis) spectra show the presence of an additional band, not seen in the individual components, that

dx.doi.org/10.1021/ic3002948 | *Inorg. Chem.* 2012, 51, 8064−8072

may be assigned to the chloranil-AB charge-transfer complex formed within the galleries of the LDH. The extent of charge transfer from the intercalated AB ion to the included chloranil determined from the shift of the vibrational frequency of the chloranil C=O bond is 0.28. Surprisingly, the inclusion of chloranil does not result in any change in the interlayer spacing from that of Mg-Al LDH-AB. Even at the highest concentration of included chloranil, the spacing remains at 15.2 Å. MD simulations of the chloranil-included Mg-Al LDH-AB showed that it is possible to include the *ortho*- and *para*-chloranil molecules without any significant change in lattice parameters. The included chloranil molecules are arranged in the galleries of the Mg-Al LDH with their molecular planes parallel to that of the intercalated AB ions.

In conclusion, we have shown how neutral chloranil molecules may be included within the galleries of a Mg-Al layered double hydroxide by using charge-transfer interactions with preintercalated *p*-aminobenzoate ions as the driving force. Although the present study was limited to the layered double hydroxides, the methods and strategy outlined here for inclusion of neutral molecules could easily be extended to other layered solids. All it requires is that the solid be functionalized by preintercalation of one of the partners of a donor−acceptor pair: chemistry does the rest.

■ ASSOCIATED CONTENT

Supporting Information

TGA profiles of Mg-Al LDH-AB, Mg-Al LDH-(AB·*p*-chloranil) and Mg-Al LDH-(AB·*o*-chloranil). Calculated atomic charges on the *p*-aminobenzoate anion and chloranil isomers. Infrared and Raman band positions and assignments for Mg-Al LDH-AB, Mg-Al LDH-(AB·*p*-chloranil) and Mg-Al LDH-(AB·*o*-chloranil). Variation of the interlayer spacing from MD simulations of Mg-Al LDH-(AB·*p*-chloranil) and Mg-Al LDH-(AB·*o*-chloranil) as function of the chloranil:AB molar ratio. This material is available free of charge via the Internet at http://pubs.acs.org.

■ AUTHOR INFORMATION

Corresponding Author

*Tel.: +91-80-2293-2661. Fax: +91-80-2360-1552/0683. E-mail: svipc@ipc.iisc.ernet.in.

Notes

The authors declare no competing financial interest.

■ ACKNOWLEDGMENTS

The authors thank Mr. T. Anil Kumar for help with the MD simulations and the Supercomputer Education and Research Centre, Indian Institute of Science for use of the computational facilities.

■ REFERENCES

(1) Bartlett, N.; McQuillan, B. W.; Whittingham, M. S.; Jacobson, A. J. *Intercalation Chemistry*; Academic Press: New York, 1982.
(2) Alberti, G.; Costantino, U.; Bein, T. *Comprehensive Supramolecular Chemistry*; Elsevier Science: London, 1996; Vol. 7, p 1.
(3) Pinnavaia, T. J.; Raythatha, R.; Lee, J. G.-S.; Halloran, L. J.; Hoffman, J. F. *J. Am. Chem. Soc.* **1979**, *101*, 6891.
(4) Duan, X.; Evans, D. G. *Layered Double Hydroxides, Structure and Bonding*; Springer−Verlag: Berlin, Heidelberg, 2006.
(5) Khan, A. I.; O'Hare, D. *J. Mater. Chem.* **2002**, *12*, 3191.
(6) Joy, P. A.; Vasudevan, S. *J. Am. Chem. Soc.* **1992**, *114*, 7792.
(7) Alberti, G.; Casciola, M.; Costantino, U.; Vivani, R. *Adv. Mater.* **1996**, *8*, 291.
(8) Mallouk, T. E.; Gavin, J. A. *Acc. Chem. Res.* **1998**, *31*, 209.
(9) Venkataraman, N. V.; Mohanambe, L.; Vasudevan, S. *J. Mater. Chem.* **2003**, *13*, 170.
(10) Venkataraman, N. V.; Vasudevan, S. *J. Phys. Chem. B* **2003**, *107*, 5371.
(11) Dutta, P. K.; Robbins, D. S. *Langmuir* **1994**, *10*, 1851.
(12) Venkataraman, N. V.; Vasudevan, S. *J. Phys. Chem. B* **2001**, *105*, 1805.
(13) Venkataraman, N. V.; Vasudevan, S. *Proc. Indian Acad. Sci., (Chem. Sci.)* **2001**, *113*, 539.
(14) Kijima, T.; Matsui, Y. *Nature* **1986**, *322*, 533.
(15) Zhao, H.; Vance, G. F. *J. Chem. Soc., Dalton Trans.* **1997**, *11*, 1961.
(16) Zhao, H.; Vance, G. F. *J. Incl. Phenom. Mol. Rec. Chem.* **1998**, *31*, 305−317.
(17) Zhao, H.; Vance, G. F. *Clays Clay Miner.* **1998**, *46*, 712.
(18) Mohanambe, L.; Vasudevan, S. *Langmuir* **2005**, *21*, 10735.
(19) Trifiro, F.; Vaccari, A.; Alberti, G.; Bein, T. *Comprehensive Supramolecular Chemistry*; Elsevier Science: London, 1996; Vol. 7, p 251.
(20) Venkataraman, N. V.; Vasudevan, S. *J. Phys. Chem. B* **2003**, *107*, 10119.
(21) Zhao, Q.; Chang, Z.; Lei, X.; Sun, X. *Ind. Eng. Chem. Res.* **2011**, *50*, 10253.
(22) Arellano-Cardenas, S.; Gallardo-Velazquez, T.; Poumian-Gamboa, G. V.; Osorio-Revilla, G.; Lopez-Cortez, S.; Rivera-Espinoza, Y. *Clays Clay Miner.* **2012**, *60*, 153.
(23) Mohanambe, L.; Vasudevan, S. *J. Phys. Chem. B* **2006**, *110*, 14345.
(24) Ogawa, M.; Kuroda, K. *Bull. Chem. Soc. Jpn.* **1997**, *70*, 2593.
(25) Wouter, L.; Pinnavaia, T. J. *Green Chem.* **2001**, *3*, 10.
(26) Chaara, D.; Bruna, F.; Ulibarri, M. A.; Draoui, K.; Barriga, C; Pavlovic, I. *J. Hazard. Mater.* **2011**, *196*, 350.
(27) Kijima, T.; Tanaka, J.; Goto, M.; Matsui, Y. *Nature* **1984**, *310*, 45.
(28) Mohanambe, L.; Vasudevan, S. *Inorg. Chem.* **2004**, *43*, 6421.
(29) Jin, L.; He, D.; Wei, M. *Chem. Eng. Technol.* **2011**, *34*, 1559.
(30) Jin, L.; Liu, Q.; Sun, Z.; Ni, X.; Wei, M. *Ind. Eng. Chem. Res.* **2010**, *49*, 11176.
(31) Liu, X. L.; Wei, M.; Wang, Z. L.; Evans, D. G.; Duan, X. *J. Phys. Chem. C* **2008**, *112*, 17517.
(32) Mohanambe, L.; Vasudevan, S. *Inorg. Chem.* **2005**, *44*, 2128.
(33) Mohanambe, L.; Vasudevan, S. *J. Phys. Chem. B* **2005**, *109*, 22523.
(34) Mohanambe, L.; Vasudevan, S. *J. Phys. Chem. B* **2005**, *109*, 11865.
(35) Mukherjee, D. C.; Chandra, A. K. *J. Phys. Chem.* **1964**, *68*, 477.
(36) Nogami, T.; Yoshihara, K.; Hosoya, H.; Nagakura, S. *J. Phys. Chem.* **1969**, *79*, 2670.
(37) Meyn, M.; Beneke, K.; Lagaly, G. *Inorg. Chem.* **1990**, *29*, 5201.
(38) Bellotto, M.; Rebours, B.; Clause, O.; Lynch, J.; Bazin, D.; Elkaïm, E. *J. Phys. Chem.* **1996**, *100*, 8527.
(39) Levashov, V. A.; Thorpe, M. F. *Phys. Rev. B* **2003**, *67*, 224109.
(40) Naik, V. V.; Chalasani, R.; Vasudevan, S. *Langmuir* **2011**, *27*, 2308.
(41) Rappé, A. K.; Casewit, C. J.; Colwell, K. S.; Goddard, W. A.; Skiff, W. M. *J. Am. Chem. Soc.* **1992**, *114*, 10024.
(42) Mayo, S. L; Olafson, B. D.; Goddard, W. A. *J. Phys. Chem.* **1990**, *94*, 8897.
(43) Newman, S. P.; Williams, S. J.; Coveney, P. V.; Jones, W. *J. Phys. Chem. B* **1998**, *102*, 6710.
(44) Newman, S. P.; Greenwell, H. C.; Coveney, P. V.; Jones, W.; Rives, V. *Layered Double Hydroxides: Present and Future*; Nova Science: New York, 2001.
(45) *Materials Studio, Version 4.4.0.0*, Accelrys Software, Inc.: San Diego, CA, 2008.

(46) Frisch, M. J.; Trucks, G. W.; Schlegel, H. B.; Scuseria, G. E.; Robb, M. A.; Cheeseman, J. R.; Scalmani, G.; Barone, V.; Mennucci, B.; Petersson, G. A.; Nakatsuji, H.; Caricato, M.; Li, X.; Hratchian, H. P.; Izmaylov, A. F.; Bloino, J.; Zheng, G.; Sonnenberg, J. L.; Hada, M.; Ehara, M.; Toyota, K.; Fukuda, R.; Hasegawa, J.; Ishida, M.; Nakajima, T.; Honda, Y.; Kitao, O.; Nakai, H.; Vreven, T.; Montgomery, Jr., J. A.; Peralta, J. E.; Ogliaro, F.; Bearpark, M.; Heyd, J. J.; Brothers, E.; Kudin, K. N.; Staroverov, V. N.; Kobayashi, R.; Normand, J.; Raghavachari, K.; Rendell, A.; Burant, J. C.; Iyengar, S. S.; Tomasi, J.; Cossi, M.; Rega, N.; Millam, N. J.; Klene, M.; Knox, J. E.; Cross, J. B.; Bakken, V.; Adamo, C.; Jaramillo, J.; Gomperts, R.; Stratmann, R. E.; Yazyev, O.; Austin, A. J.; Cammi, R.; Pomelli, C.; Ochterski, J. W.; Martin, R. L.; Morokuma, K.; Zakrzewski, V. G.; Voth, G. A.; Salvador, P.; Dannenberg, J. J.; Dapprich, S.; Daniels, A. D.; Farkas, Ö.; Foresman, J. B.; Ortiz, J. V.; Cioslowski, J.; Fox, D. J. *Gaussian 09 Program*; Gaussian, Inc.: Wallingford, CT, 2009.
(47) Jorgensen, W. L.; Chandrasekhar, J.; Madura, J. D.; Impey, R. W.; Klein, M. L. *J. Chem. Phys.* **1983**, *79*, 926.
(48) Woodcock, L. V. *Chem. Phys. Lett.* **1971**, *10*, 257.
(49) Prevot, V.; Forano, C.; Besse, J. P. *Appl. Clay Sci.* **2001**, *18*, 3.
(50) Masino, M.; Girlando, A.; Brillante, A. *Phys. Rev. B* **2007**, *76*, 064114.
(51) Ranzieri, P.; Masino, M.; Girlando, A. *J. Phys. Chem. B* **2007**, *111*, 12844.
(52) Girlando, A.; Zanon, I.; Sozio, R.; Pecile, C. *J. Chem. Phys.* **1978**, *68*, 22.
(53) Tokura, Y.; Okamoto, H.; Koda, T.; Mitani, T.; Saito, G. *Solid State Commun.* **1986**, *57*, 607.